MÄLARDALEN UNIVERSITY
SCHOOL OF INNOVATION, DESIGN AND ENGINEERING
VÄSTERÅS, SWEDEN

CEL405 Project in Electronics 15.0 hp

INTEGRATING PASS THROUGH CHARGING IN A SOLAR CAR BY USING A POWERPATH CONTROLLER

Syafirul Ariff bin Selimin
sbn17010@student.mdh.se

Examiner: Martin Ekström
Mälardalen University, Västerås, Sweden

Company Supervisor: MDH Solar Team
solarteam@mdh.se

10 August 2018

Abstract

In October 2019 the MDH Solar Team will compete in the Adventure Class of the Bridgestone World Solar Challenge held in Australia every second year. This project focuses on transferring power from the two available power sources permitted during the competition, solar and a rechargeable battery to the engine of the car. The idea is to implement pass through charging in the circuitry of the solar car's battery. In simple terms, pass through charging is an integrated technology in power banks that allows a device, say a smartphone, to be plugged and charged while the power bank itself is connected to a wall outlet. This method has been used widely by power bank manufacturers to charge portable electronic devices. However, it is not known to date if the technology has been used in electric cars. Although it has been used widely in the portable electronics field, the implementation is not as direct as it may seem. Car batteries are much more complex, and they possess more physical challenges that may easily interfere with the micro electronics. Since no battery manufacturer for the solar car is able to work together with the author in building the battery, a custom circuit board has to be made. One powerpath controller and two dual p-channel MOSFETs are used in the circuit. This circuit board will be the intermediate between the two power sources and the engine. The developed circuit board is tested on its possibility and reliability to see whether it can be used on a car's battery.

Table of Contents

1. Introduction

Mälardalen University (MDH) has a group of students working on a solar car that was built and designed entirely from scratch by them. Originally, the idea of this student project was born back in 2014 from the minds of a few students under the M.Sc. Engineering program in Production and Product Design, with the goal of competing in the 2017 Bridgestone World Solar Challenge [1]. The objective of this competition is to promote research on solar-powered cars. Teams from universities and enterprises participate every second year in Australia. In 2017, the competition welcomed 42 entrants from 19 countries that raced from Darwin in the Northern Territory and finished in the City of Adelaide in South Australia for a total of 3021km. The competition hosts three classes that represent the diversity of solar cars and their differing design philosophies.

Since then, some 70 students from MDH have worked with the car under the team's official name, MDH Solar Team. These students have worked by themselves under the supervision of lecturers from the university. Driven by their high interests and eagerness, they managed to put up a solar powered car just in time for the race to compete under the Adventure class. The Adventure Class is non-competitive and allows cars built for previous editions of the event to run again, usually with new team members. It can also be used as a catchment for those who, while meeting the exacting safety standards, may not have quite made full compliance with the latest requirements. During the race, the MDH Solar Car experienced some critical power loss. After some diagnosis the team found out that there was some current leak between the MPPT's and the battery. However, that did not prevent the team from finishing the race, positioning themselves 5th out of 23 competitors.

The problem that they had rose a question in my head; what if pass through charging is used instead? This method has been used widely by power bank manufacturers to charge portable electronic devices. In simple terms, pass through is an integrated technology in power banks that allows a device, say a smartphone, to be plugged and charged while the power bank itself is connected to a wall outlet. *Pass through technology itself is in essence a series of power regulating circuits inside a power bank that helps match the draw of energy needed by an output device to the amps being pulled from a wall outlet. If done right, pass through will move power directly from the wall outlet to the connected device, via the power bank* [2]. This is called prioritization. Depending on load balancing performance in the power bank, the latter should charge at either a regular or slower speed than normal when working with an output device.

Since the base of this pass-through technology is essentially the same for every electrical circuit, where the connection is in series resulting in, power outlet → power bank → electronic device, the same can be applied for the car where the connection is solar panels → battery → engine. To implement this idea, the battery needs to be charged and discharged from two separate cables.

The idea was discussed thoroughly with the electronics department of the solar team. However, the idea can't be implemented due to restrictions by the sponsor of the battery. They do not allow any alterations to be done to the battery. There were also other barriers from carrying out the test on the car's 120V 4800Wh Lithium Ion battery. After the race ended, the battery is believed to have self discharged under the minimum cell voltage of 2.5V. The battery could not operate, preventing the solar car from starting.

The best way to implement this idea is to test it on the mini autonomous solar car (from here onwards referred as MASC). This is a summer project being carried out by a group of nine M.Sc. Engineering in Robotics students under the project title "Mini Autonomous Solar Team (MAST)" [3]. This project was born due to the interest of the main sponsor Volvo in converting the MDH Solar Car to become autonomous. MASC is a miniaturized replica of the current solar car with a scale of 1:6. The aim of MAST is to build and implement hardware and software of the solar car to convert it into an autonomous solar car. The MASC requires a Litihium Polymer battery as its power source. Therefore, the focus of this project will be on applying this technology on this kind of battery, although it is believed that it can be used on other kinds of batteries as well.

2. Background

The MASC is built around a National Instruments' (NI) RoboRIO which allows for fast prototyping and easy interaction with I/O. The RoboRIO is used as the basis for the control system and will manage velocity and steering, but also monitoring the status of the battery. In order to get the autonomous behaviour, one Nvidia Jetson TX2 is used with three range detecting sensors and a camera for mapping and localization on the track. The idea is to keep the TX2 separate from the RoboRIO in such a way that the car can be controlled remotely without any changes to the software on the RoboRIO. In order to achieve adequate velocity and considering the estimated weight of 20kg an obvious desire is to reduce the transmission power loss as much as possible, hence using directly mounted motors inside each wheel is an appropriate solution. Another crucial thing that is taken into consideration is to make sure the vehicle is stable and fairly mobile in both low speed and high-speed applications, thus a 4WS system is an appropriate solution. The mini car should be able to reach 70km/h or faster, just like the original solar car. Below is a figure of how all the electronic peripherals are connected.

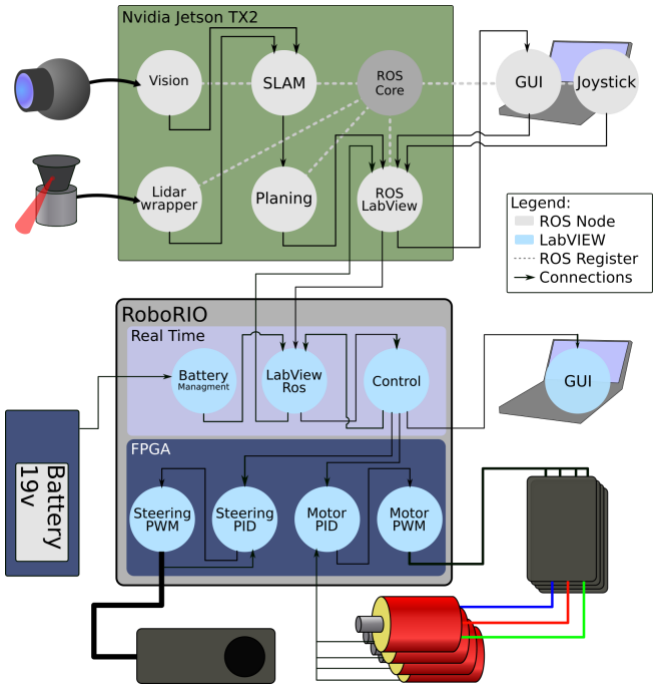

Figure 1: Functional diagram of the MASC; note that the battery should be a 14.8V cell

NVIDIA Jetson TX2 [4] is an embedded system-on-module (SoM) and it is the fastest, most power-efficient embedded AI computing device. It is built around an NVIDIA Pascal™-family GPU and loaded with 8 GB of memory and 59.7 GB/s of memory bandwidth. It features a variety of standard hardware interfaces that make it easy to integrate it into a wide range of products and form factors. Useful for deploying computer vision and deep learning, the Jetson TX2 runs Linux and requires less than 7.5W of power.

The roboRIO Advanced Robotics Controller [5] is a reconfigurable robotics controller that includes built-in ports for I2C, serial peripheral interface (SPI), RS232, USB, Ethernet, PWM, and relays. It features LEDs, buttons, an onboard accelerometer, and a custom electronics port. The RoboRIO meets industrial shock and vibration standards. It is used mainly to control common sensors and actuators used in advanced robotics applications. It is programmable via the NI LabVIEW™.

Robot Operating System (ROS) [6] is a BSD-licensed system for controlling robotic components from a PC. A ROS system is comprised of a number of independent nodes, each of which communicates with the other nodes using a publish/subscribe messaging model. For example, a particular sensor's driver might be implemented as a node, which publishes sensor data in a stream of messages. These messages could be consumed by any number of other nodes, including filters, loggers, and also higher-level systems such as guidance, pathfinding, etc. Running sets of ROS-based processes are represented in a graph architecture where processing takes place in nodes that may receive, post and multiplex sensor, control, state, planning, actuator and other messages. To some extent it can also be defined as a robotics middleware (i.e. collection of software frameworks for robot software development).

The LTC4417 [7] is a powerpath controller that connects one of three valid power supplies to a common output based on priority. Priority is defined by pin assignment, with V1 assigned the highest priority and V3 the lowest priority. A power supply is defined as valid when its voltage has been within its overvoltage (OV) and undervoltage (UV) window continuously for at least 256ms. If the highest priority valid input falls out of the OV/UV window, the channel is immediately disconnected, and the next highest priority valid input is connected to the common output. It is typically used in servers and computer peripherals where the system needs continuous power in case of blackouts. The LTC4417 incorporates fast non-overlap switching circuitry to prevent both reverse and cross conduction while minimizing output droop. The gate driver includes a 6V clamp to protect external MOSFETs. A controlled output ramp feature minimizes start-up inrush current. Open drain VALID outputs indicate the input supplies have been within their OV/UV window for 256ms. This chip combined with a custom circuit board will be tested on the MASC.

A multi-input power system has switches multiplexing the input supplies to a common output load. A Powerpath controller [8] is basically what the name hints—it selects and controls the path on which power flows to the system. The controller selects the input source based on highest voltage or highest priority; the former type is called an ideal diode, while the latter is called a prioritizer. Powerpath controllers employ integrated or external, single or back-to-back, P- or N-channel MOSFET switches to multiplex up to three input supplies to the common output load. More than three supplies are multiplexed by employing multiple controllers.

Voltage droop [9] defines the loss in output voltage from a device as it tries to drive a (capacitive) load. The reduction out voltage level may or may not be an issue depending on the circuit in question. For example, if the receiving IC is a digital logic IC the level reduction might not even be noticed if the final value never falls below a transition point. Not supplying sufficient current to an IC that needs to drive a heavy load is one example that could cause voltage droop. Increasing the value of the by-pass capacitor used by the IC is a possible fix. The value of the Decoupling Capacitor that should be used with an IC depends on the load the IC has to drive. To some extent, the larger the decoupling capacitor used with the IC, the larger the load the IC will be able to drive; because the decoupling capacitor supplies current to the IC as it switches. Another solution to this would be placing a series resistor is included between the regulator output and the load. Although it may seem counterproductive, the resistance needs to be chosen so that at maximum output current, the output voltage at the load is the minimum acceptable. Conversely, when the output current is (near) zero, the voltage is near the maximum. This follows simply from Ohm's law. Note that this should not be confused with the term voltage drop, which is also present in the project.

Inrush current [10] is the instantaneous high input current drawn by a power supply or electrical equipment at turn-on. This arises due to the high initial currents required to charge the capacitors and inductors or transformers. The inrush current is also known as the switch–on surge, or the input surge current. At turn-on, the discharged capacitors in power supplies offer low impedance that allows high currents to flow into the circuit as they charge from zero to their maximum values. These currents can be as high as 20 times the steady state currents. Even though it only lasts for about 10ms it takes between 30 and 40 cycles for the current to stabilize to the normal operating value. If not limited, the high currents can damage the equipment in addition to producing voltage dips in the supply line and causing malfunctioning of other equipment powered from the same supply.

A lithium polymer battery [11], or more correctly lithium-ion polymer battery (abbreviated as LiPo, LIP, Li-poly, lithium-poly and others), is a rechargeable battery of lithium-ion technology using a polymer electrolyte instead of a liquid electrolyte. High conductivity semisolid (gel) polymers form this electrolyte. These batteries provide higher specific energy than other lithium battery types and are used in applications where weight is a critical feature, like mobile devices and radio-controlled aircraft. Just as with other lithium-ion cells, LiPos work on the principle of intercalation and de-intercalation of lithium ions from a positive electrode material and a negative electrode material, with the liquid electrolyte providing a conductive medium. To prevent the electrodes from touching each other directly, a microporous separator is in between which allows only the ions and not the electrode particles to migrate from one side to the other Lithium polymer cells have evolved from lithium-ion and lithium-metal batteries. The primary difference is that instead of using a liquid lithium-salt electrolyte (such as LiPF6), the battery uses a solid polymer electrolyte (SPE). A typical cell has four main components: positive electrode, negative electrode, separator and electrolyte. The separator itself may be a polymer, such as a microporous film of polyethylene (PE) or polypropylene (PP); thus, even when the cell has a liquid electrolyte, it will still contain a "polymer" component. In addition to this, the positive electrode can be further decomposed in three parts: the lithium-transition-metal-oxide (such as LiCoO2 or LiMn2O4), a conductive additive, and a polymer binder of poly(vinylidene fluoride) (PVdF). The negative electrode material may have the same three parts, only with carbon replacing the Lithium-metal-oxide. As mentioned before, the MASC will be using this kind of battery, as compared to Lithium Ion which is used in the MDH Solar Car.

3. Related Work

In 2017 a group of five students conducted a project under the title "Solar Challenge 2017" [12]. The project focuses on the electrical design of the MDH Solar Car both in term of hardware and software, according to the 2017 Bridgestone World Solar Challenge rules & regulations. A solar power model was made with the purpose to give an idea of the amount of solar power that can be used during the race. To maximize efficiency, mathematical model op-timization were used. Firstly, a mathematical model estimates available solar power, depending on time and location. Secondly a model of race conditions and solar car were utilized to predict/optimize power consumption.

Another related work to this project is "Optimal Load Sharing Strategy in a Hybrid Power System" [13] done by students from NTNU, Norway. They have developed an effective load sharing and control strategy for a PV/FC/Battery/Supercapacitor hybrid power system that optimizes availability, performance, fuel economy and safety. The simulation results show that the control strategy is effective in meeting high degree of power availability, and reduced cycling of battery. The battery is also relieved from steep charging currents by slightly delaying the current reference improving charging efficiency and enabling the supercapacitor efficiently to take the steep currents. A near full controllability of battery, supercapacitor and fuel cell enables operation of the units within safe limits in addition to making it possible to shape the trajectories of their power responses. The aim of this project is directly related to my thesis at it reduces the battery cycles by improving the charging efficiency.

In February 2000, a research paper was presented at the 15th Annual IEEE Applied Power Electronics Conference and Exposition entitled "Analysis, design, and performance evaluation of droop current-sharing method" [14]. This paper focused on analysing the droop current sharing method, proposing a general design procedure. Their discovery has shown that the current-sharing accuracy of N+1 power supply is a function of the output-voltage set-point accuracy, the slope of the output-voltage droop, and gains of the control loop. It was found that to achieve a current sharing accuracy of 10% the output voltage of the paralleled power supplies needs to be set within 0.35%. The accuracy of the design procedure was compared against measured results of three power supplies operating in parallel.

4. Problem Formulation

Since no battery manufacturer for the car is able to work together with the author in building the battery, a custom circuit board has to be made. This causes the writer to question himself; is it possible to implement this technology together with a car battery? Although it has been used widely in the portable electronics field, the implementation is not as direct as it may seem. Car batteries are much more complex, and they possess more physical challenges that may easily interfere with the micro electronics. After some studies it is summarized that an integrated circuit from Linear Technology (LTC) can be used as the suitable powerpath controller in the custom circuit. The LTC4417 comes in a form of surface mount device (SMD). The author however has no previous knowledge of manufacturing printed circuit boards (PCB) or dealing with SMD.

The task is to build a custom circuit board that will house the LTC4417 powered by two different power sources, with one being the wall outlet and the other being the battery, hence emulating the real environment faced by the solar car. As mentioned before, the LTC4417 has three input pins with three levels of priority. However, it can be used for dual channel operation, leaving the third channel unused or operated as a voltage regulator. A careful research was made on how to operate the LTC4417 as a dual channel powerpath controller, leaving the third channel unused. The third channel is chosen to be left unused as it would require less time and budget to suit the scope of this project. In addition to that, car batteries have their own voltage regulator.

A general guideline was made for this project. Figure below shows a block diagram of how the planned circuitry will be used together with the MASC.

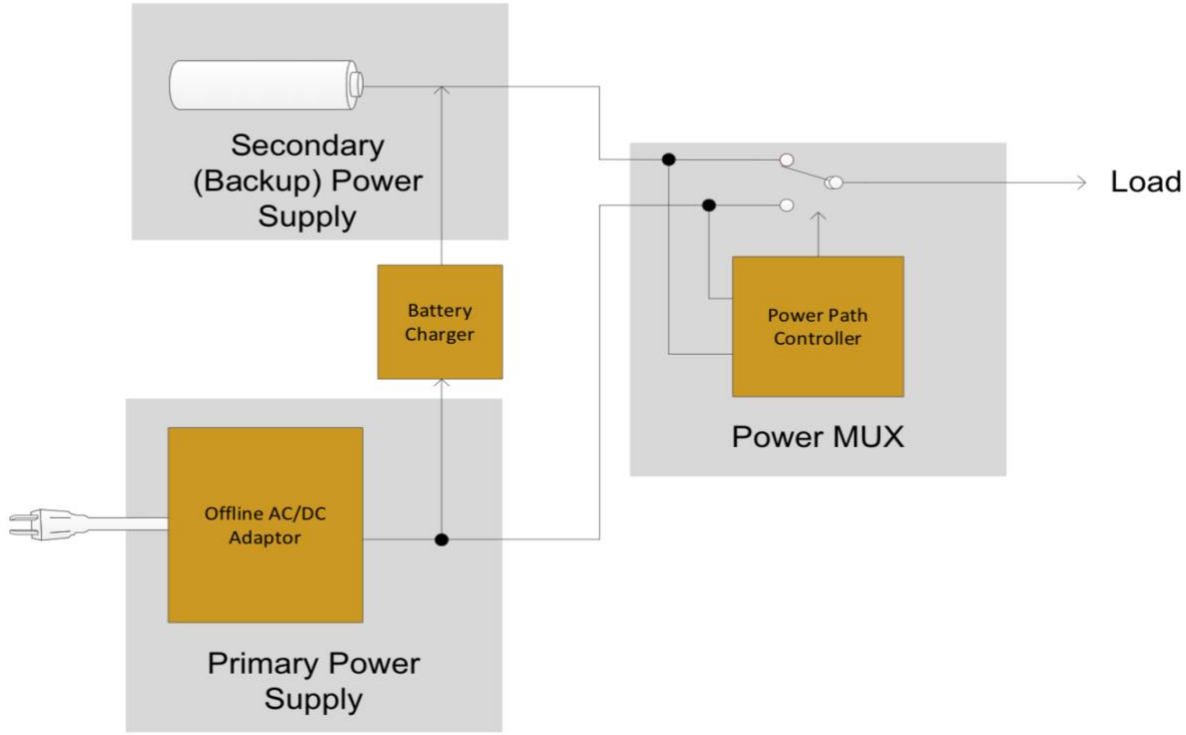

Figure 2: Block diagram of the proposed circuitry

5. Methods and Calculations

One of the main uses of the LTC4417 is for battery backup systems. To fully understand how it works, simulations have to be made. It requires the author to run a simulation by using LTSpice, an open source analog electronic circuit simulator implementing simulation program with integrated circuit emphasis. A better option would have been Multisim since it has a direct integration with Ultiboard. Nevertheless, it can not be used to simulate the LTC4417. It is understood that the LTC4417 is more of an industrial grade IC that is very well patented and protected. A planning was done by defining how the experiment should be carried out and under what cirscumtances. A predefined parameter of both voltage inputs was done before selecting each and every component that will be used in the circuit. This is important in order to facilitate the order of components before constructing the circuit and carrying out the tests in real life.

A 2A rated dual input supply system consisting of a 14V power supply and a 14.8V (nominal voltage) LiPo battery with a source resistance, R_{src} of 20mΩ is designed with priority sourcing from the 14V power supply. Power is sourced from the battery when the 14V power supply is absent. And with the use of LTC4417, it allows the input to be changed back to the power supply when the battery is running low. The ambient conditions of the system will be 25°C. The design limits the output voltage droop to 800mV during switchover. The input source is allowed to drop 1V.

5.1 Selecting P-channel MOSFETs

There have to be two dual P-channel MOSFET to conduct or block load current between an input supply and load. To select the P-channel MOSFETs, the key parameters to consider are on-resistance ($R_{DS(ON)}$), absolute maximum rated drain to source break-down voltage ($BV_{DSS(MAX)}$), threshold voltage ($V_{GS(TH)}$), power dissipation, and safe operating area (SOA). To determine the required ($R_{DS(ON)}$), equation (1) is used where V_{DROP} is the maximum desired voltage drop across the two series MOSFETs at full load current, $I_{L(MAX)}$, for the application. It is known that the clamped gate drive output is 4.5V (minimum) from the common source connection.

$$\left(R_{DS(ON)}\right) \leq \frac{V_{DROP}}{2 \times I_{L(MAX)}} = \frac{1000mV}{4A} = 250m\Omega \qquad \text{Equation (1)}$$

The design starts with selecting a suitable 2A rated P-channel MOSFET with desired RDS(ON). Reviewing several MOSFET options, the low 105mΩ $R_{DS(ON)}$, dual P-channel IRF7342 with a –55V BV_{DSS}, is chosen for this application. The low 105mΩ $R_{DS(ON)}$ results in a 420mV drop at 25°C. Each P-channel MOSFET dissipates 72mW at 25°C.

5.2 Inrush current limiting

When connecting a higher voltage source to a lower voltage output, significant inrush current can occur. The magnitude of the inrush current can be calculated where $V_{out(init)}$ is the V_{out} voltage when initially powered from a supply voltage less than V2, since V2 is the higher voltage source, R_{src} is source resistance of V2, ESR_{CL} is the ESR of the load capacitor, and $R_{DS(ON)}$ is the on-resistance of the external back-to-back MOSFET. Given a total series resistance from input to output, the worst-case inrush current will occur when V2 is running at full capacity, and V_{out} is at its undervoltage limit of 12V. During this condition, a maximum inrush current of 10A will occur, as shown in equation (2).

$$I_{inrush} = \frac{V2 - V_{out(init)}}{R_{src} + ESR(CL) + 2 \times R_{DS(on)}} = \frac{14.8V - 12V}{20m\Omega + 50\text{m}\Omega + 210\text{m}\Omega} = 10A \qquad \text{Equation (2)}$$

Calculating the load capacitance, C_L is an iterative process. To start, limit the output voltage droop to the desired 800mV, reserve 200mV for initial droop due to the load current flowing in the ESR of the output capacitor. Next, choose C_L to set the maximum V_{out} droop to 600mV, as shown in equation (3).

$$C_L = \frac{2A \times 25\mu s}{600mV} = 83.8\mu F \qquad \text{Equation (3)}$$

For margin, the initial C_L value is chosen to be equal to 100µF. With an allowable 1V input voltage drop and source resistance of 20mΩ, the input voltage droop of 700mV is used to set the inrush current of 10A. The other terms in the equation come from the external P-channel MOSFET manufacturer's data sheet. The transfer characteristics curve shows the gate voltage, V_{GS}, is approximately 1.8V when driving the 10A inrush current and the capacitance verses drain-to-source voltage curve shows the maximum C_{RSS} is approximately 600pF. C_S is set to be greater than ten times C_{RSS}, or 6.8nF. To ensure the designed inrush current is lower than the absolute maximum pulse drain current rating, I_{DM}, calculate R_S using the maximum value for $\Delta V_{G(SINK)}$ and C_L, and the minimum value for C_S. C_{VS1} is chosen to be ten times C_S or 68nF.

$$R_s = \frac{6V - 1.8V \times 120\mu F \times 20m\Omega}{6.5nF \times 700mV} = 2.22k\Omega$$ Equation (4)

With R_s and C_s known, the desired load capacitance with inrush current limiting is checked. Because the required load capacitance of 90µF is lower than the chosen load capacitor of 100µF, the initial choice of 100µF is suitable.

$$C_L = \frac{2A \times (3\mu s + 12\mu s + 0.79 \times 2.22k\Omega \times 6.8nF)}{600mV} = 90\mu F$$ Equation (5)

Significant power is dissipated during the channel transition time. The SOA of the P-channel MOSFETs was checked to make sure their SOA is not violated. Worst case slew rate limited channel transition time would occur when the LiPo battery is running low at 12V. This results in a time of 25µs.

5.3 Defining operational range

To guard against noise and transient voltage events during live insertion, the LTC4417 requires an input supply remain in the overvoltage/undervoltage window for at least 256ms to be valid. The OV/UV window for each input supply is set by a resistive divider (for example, R1, R2 and R3 for V1 input supply) connected from the input supply to GND. While setting the resistive divider values for the OV and UV input supply threshold, the tolerance of the input supply was taken into consideration, with 1.5% error in the OV and UV comparators, tolerance of R1, R2 and R3, and the ±20nA maximum OV/UV pin leakage currents. In addition to tolerance considerations, hysteresis reduces the valid input supply operating range. Input supplies will need to be within the reduced input supply operating range to validate. V1 supply voltage must be greater than UV_{HYS} to exit the UV fault. If an OV fault occurs, the V1 supply voltage must return to a voltage lower than the OV_{HYS} voltage to exit the OV fault. The LTC4417 provides an 8µs OV/UV fault filter time.

Assuming the 14V source has a tolerance of ±20%, the input source has an operational undervoltage limit of 11.2V and an overvoltage limit of 16.8V. Ideally the UV1 and UV2 and OV1 and OV2 thresholds would be set to these limits. However, since the actual threshold varies by 1.5% and resistor tolerances are 1%, OV and UV limits must be adjusted to ±26% or 10.4V and 17.6V. A fixed 30mV of internal hysteresis for the OV and UV comparators are set via the HYS pin connected to GND. The following value of resistors are calculated then using equation (6), equation (7), equation (8) and equation (9).

$$R3 = \frac{Hysterisis}{I_{OVUV(HYS)}} \times \frac{30mV}{37nA} = 806k\Omega \approx 802k\Omega$$ Equation (6)

$$R1, R2 = \frac{R3}{UV_{TH(FALLING)} - V_{OVUV(THR)}} = \frac{806k\Omega}{10.4V - 1V} = 86k\Omega$$ Equation (7)

With that, R1 is

$$R1 = \frac{R1, R2 + R3}{UV_{TH(RISING)}} = \frac{86k\Omega + 806k\Omega}{17.6V} = 51k\Omega \approx 55.7k\Omega$$ Equation (8)

R2 is

$$R2 = R1, R2 - R3 = 51k\Omega \approx 30.3k\Omega \approx 39.4k\Omega$$ Equation (9)

To calculate the values of R4, R5 and R6, the same steps above are repeated. This give values of 55.7kΩ, 26.8kΩ and 845kΩ respectively.

6. Designing the circuit

All calculations were done and studied thoroughly. The final circuit was achieved and drawn on LTSpice. As suggested by the manufacturer, the four pins (VALID3, EN, SHDN and CAS) are to be left open since they are not used. Pins for the unused third channel (V3, UV3, OV3, VS3 and G3) are grounded. Connections of the dual-channel MOSFETs are done based on the manufacturer's advice. Figure below shows the circuit.

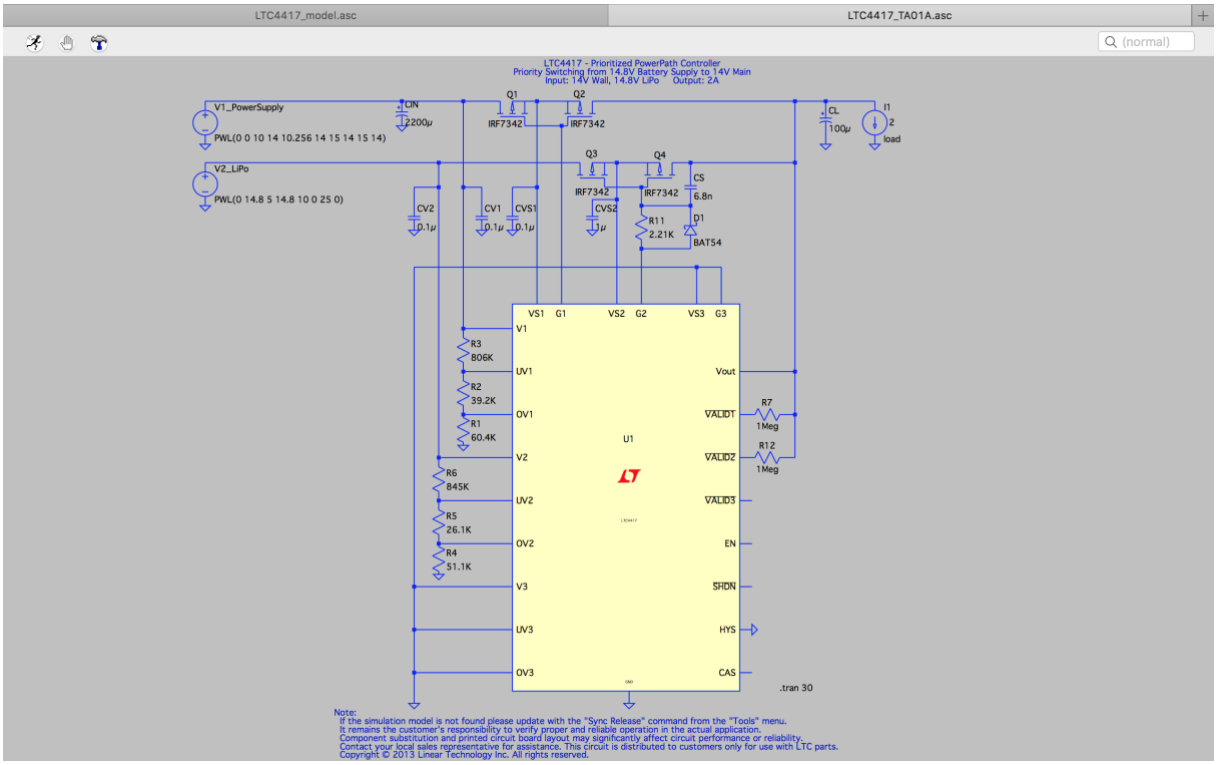

Figure 3: Circuit constructed on LTSpice for simulation purpose

After a run of successful tests on the software, the author decided to proceed with building the physical circuit board. Some of the electronic components were ordered while some were already available in the robotics laboratory. Most of the components chosen are though hole technology (THT) as the author has more on-hand experience with them. A vigorous planning was vital at this stage of the project. This is because the author has never fabricated a printed circuit board (PCB) at the university, where the author spent one year as an exchange student. Small steps such as ordering the components took time, especially because the main electronic supplier of the university, Microkit AB was closed during the summer. The order of components had to be done from other dealers.

The first step was to duplicate the circuit from LTSpice to Multisim. This is because the Multisim houses the capability of exporting the circuit to Ultiboard, where the PCB layout will be designed. However, Multisim does not have the LTC4417 in its database. Hence, to complete the circuit in Multisim a custom component of the LTC4417 has to be created on Ultiboard beforehand. Once it is done, the custom component can then be saved on the Ultiboard database, and then exported to Multisim database. This took some significant time off the project. The figure below shows the custom LTC4417 with measurements taken from the GN package. Measurements were done in mm and mil.

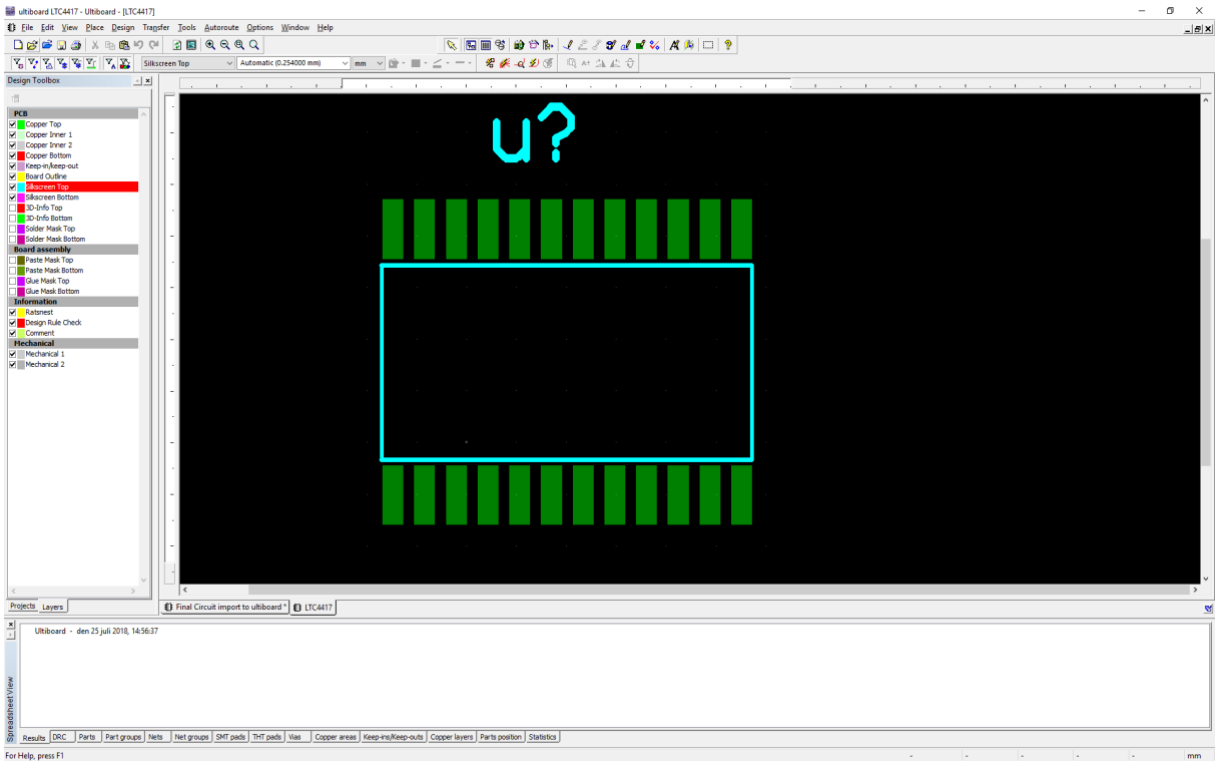

Figure 4: The custom LTC4417 in Ultiboard

The figure below shows the duplicated circuit in Multisim. Consider that this is the most ideal circuit that should be constructed. Which means that all component values are marked with the calculated theoretical values.

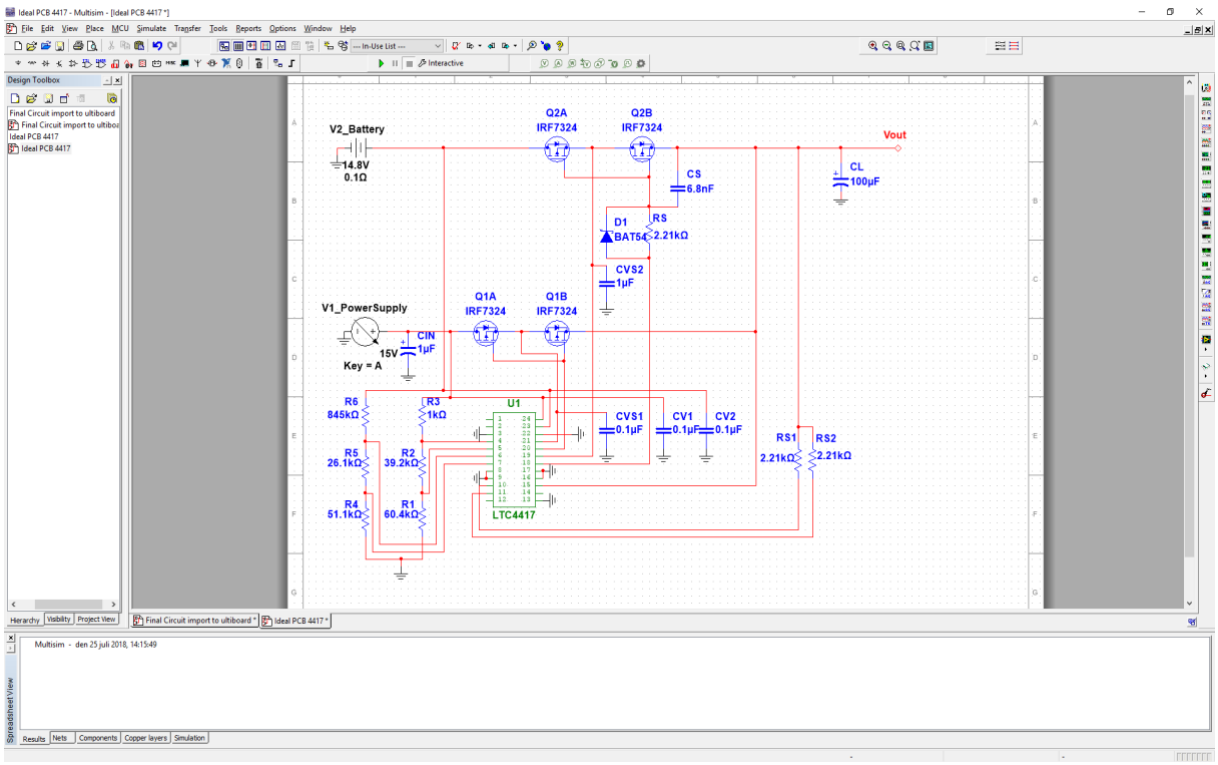

Figure 5: Multisim circuit with all the manufacturers specifications

Due to some circumstances, the final circuit was altered a little since some of the components could not be found in the laboratory. For example, some resistors are labelled with R1a and R1b and placed in series in order to get the closest value as possible to R1. Other changes made are R3a + R3b = R3, R6a + R6b = R6, R10a + R10b = R10, R11a + R11b = R11, and RSa + RSb = RS. C_{IN1} is changed to 2.2µF. Figure below is the final circuit before being exported to Ultiboard for further design of the PCB.

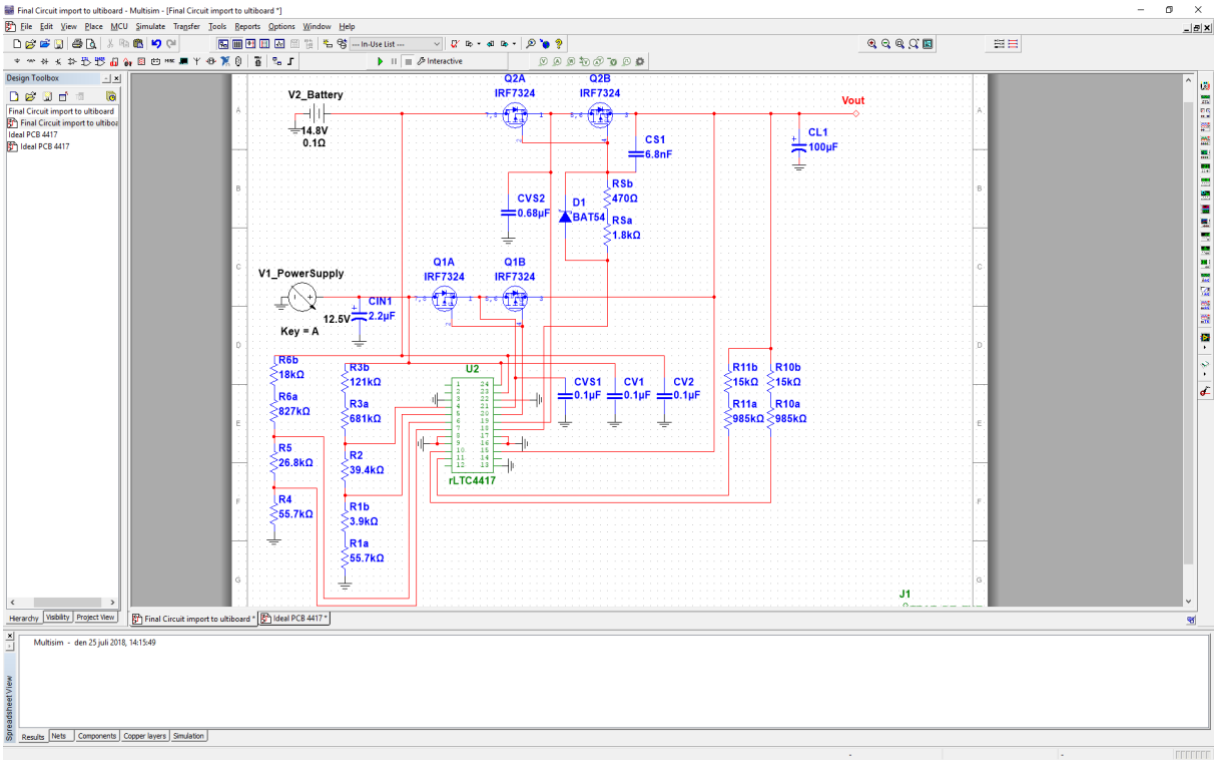

Figure 6: Final circuit in Multisim with the available components

After the circuit was exported to Ultiboard, all the components were arranged based on the recommendation of the PCB layout by the manufacturer. Upon further inspection, the voltage in and out were not exported in the process. The author decided to use a standard two pin screw on connectors for all three connections (V1, V2 and Vout). This type of connector was chosen because it was readily available on the laboratory and it fits well with the usage later on. It allows rapid connect and disconnect of the wires without damaging the board. This however required the connectors to be customly created on Ultiboard. The same process was repeated from the design of LTC4417 on Ultiboard.

Some further redesigning was needed for the layout of the circuit, hence taking up some more significant time for this part of the project. It was also taken into consideration that the circuit should be small for various reasons; the first is to reduce the amount of resistance caused by the copper traces of the PCB, considering that the sheet resistance of 1oz of copper is ≈ 530µΩ per square. Although small, resistances add up quickly in high current applications. The copper traces were kept as short as possible and with a width of 0.254mm. To improve noise immunity, the OV/ UV resistive dividers were placed as close to the LTC4417 as possible. The second reason being that this circuit is supposed to be able to fit inside the MASC's battery. However, the practicality should not be compromised as this is mainly a prototype that will require further refinements in the future. The final design has copper wires being printed on the top and bottom layer. The figure below shows the final layout of the PCB on Ultiboard.

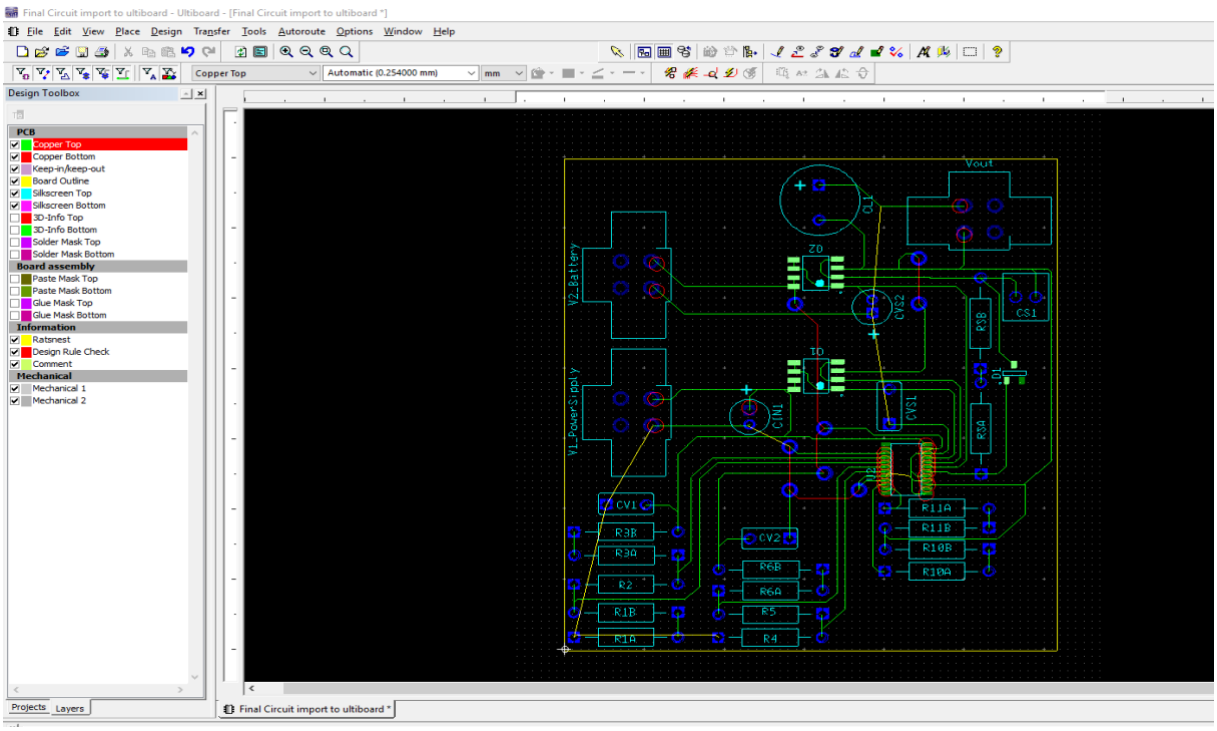

Figure 7: Final look of the circuit exported to Ultiboard before being printed

The components were all at hand before the PCB was printed. Once the PCB was printed, one by one component was soldered, starting with the LTC4417 as the main component, and finished off with the screw on connectors. a short circuit test was conducted between all connections. The following image is the actual PCB with the connectors strapped on and off.

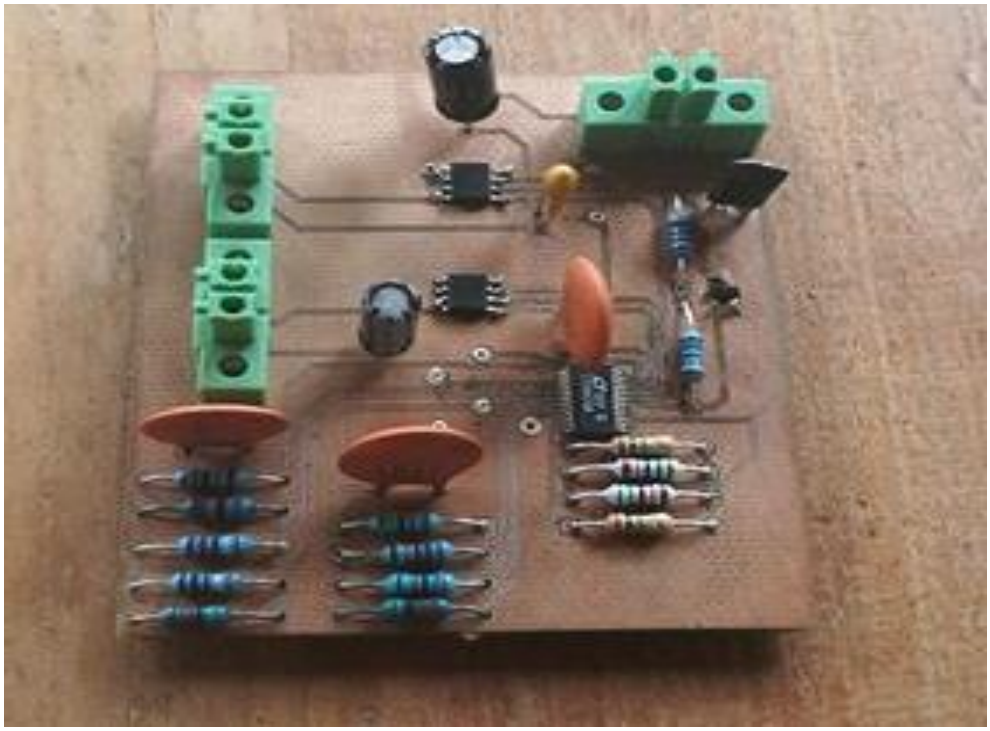

Figure 8: PCB with connectors off

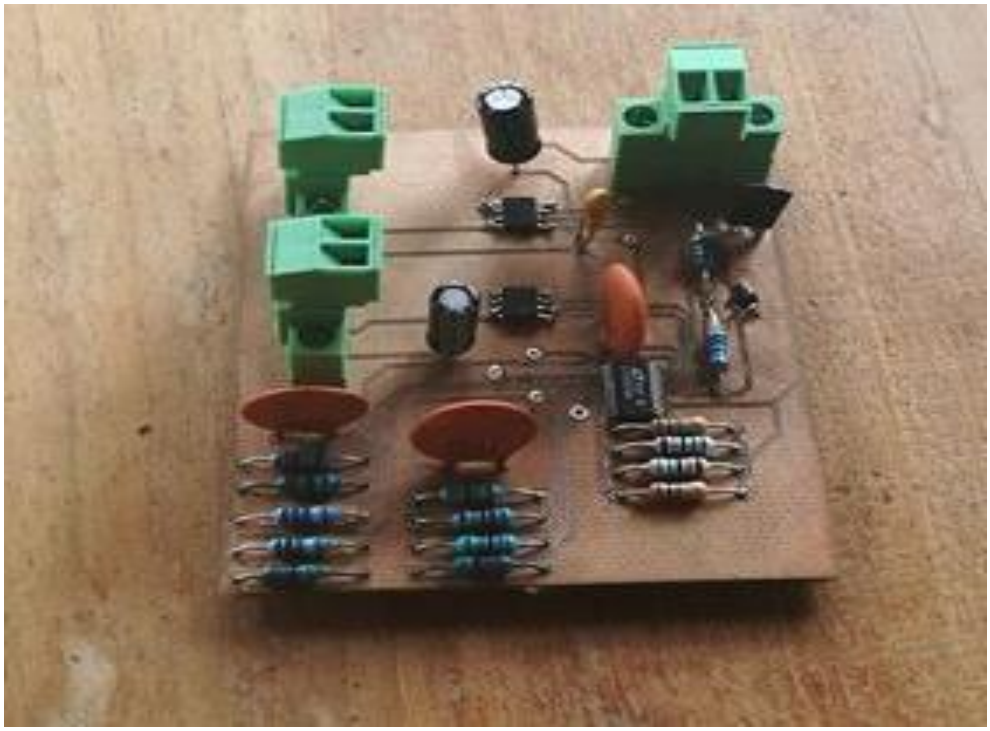

Figure 9: PCB with connectors on

7. Results

The author tested the PCB with the two available power sources, V1 being a Rohde&Schwarz HMC8043 three channel power supply from the laboratory and V2 being the Turnigy 5000mAh 4S 25C-35C 14.8V LiPo battery pack.

The power supply has a maximum total power of up to 100W and a continuous voltage range from 0V to 32V and a maximum of 3A per channel. All three outputs are galvanically isolated, floating, and protected against overloading and short circuits. Not much is known about the LiPo battery besides from what is found on the basic specification sheet. The internal resistance as mentioned before was assumed to be 20mΩ.

During the tests, both power sources were connected to the PCB at all times. The digital multimeter on the other hand was connected in different points of the circuit. The author used three channels of the multimeter with each of them being connected to V1, V2 and Vout respectively. Each of these channels were automatically assigned with different names by the multimeter in each case. Two situations were tested with the circuit as it involves switching back and forth from two different power sources.

CASE 1: Switching from power supply to battery

The first one being switching from power supply to battery, so to say from V1 to V2. In real life, this situation would occur when the solar cells are not generating enough energy to power up the car, hence relying fully on the car's battery. This will allow the solar cells to charge the battery even when the energy generated is low. Some specific environments were set for this test. Firstly, the power supply must maintain a stable value of 14V dc and 2A maximum current. To ensure this the power supply was set at constant voltage (CV) mode. The power supply also has an electronic fuse function which allows it to be triggered, thus deactivating the supply. The intent is to prevent damage to the circuit in case an error occurs (e.g. a short circuit). The LiPo battery was assumed to be at nominal capacity during the test, providing a stable 14.8V dc.

The author tested the flow of current between V1 and Vout and V2 and Vout separately before connecting both of them at the same time to the circuit. After all tests were clear and deemed satisfied by the author, the experiment began. After a few seconds, V1 was disconnected to simulate the situation when the solar cells are losing immediate power. This is when the battery kicks in and acts as the main energy provider. The readings were measured with a Fluke 45 digital multimeter. Note that V1 (green), V2 (blue) and Vout (red).

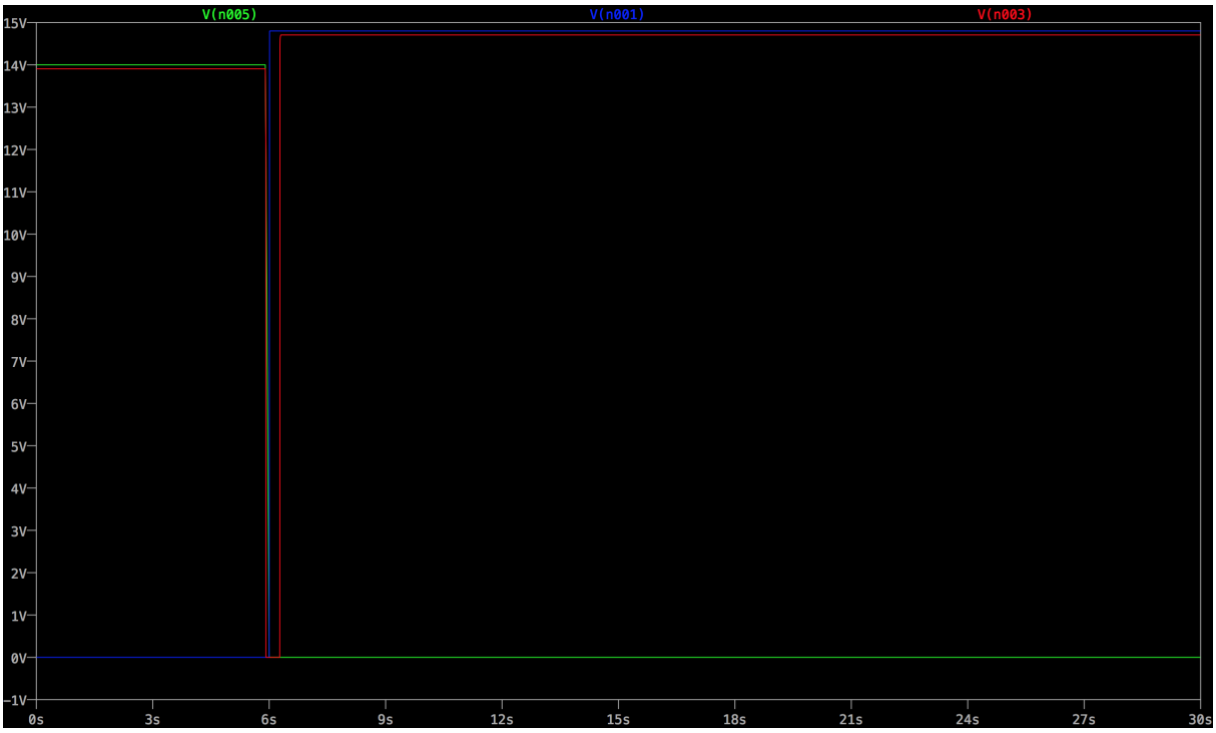

Figure 10: Line graph of the resulting switch from power supply to battery

After some interpolations and interpretations of the data, a line graph was created for all three measured voltages. A closer look at the graph indicates that Vout pulled out less voltage than V1 and V2 during the whole test. When V1 was disconnected at about 5.95s, there was a serious voltage droop in Vout that caused it to drop to 0V for approximately 200ms. The battery kicked in as soon as the LTC4417 detected that V1 was out of the defined operational range or undervoltage. Upon closer inspection it took about 150ms for the powerpath controller to accept the battery as a valid input. This means that there was approximately a 50ms buffer time in between the switching of the inputs.

CASE 2: Switching from battery to power supply

The second case will be from the LiPo battery to the power supply, or from V2 to V1. For a direct comparison, this is when the solar panels have regained enough energy from the sun to power up the car. Leaving the battery unused to conserve energy. This can the battery to be charged by the leftover energy from the solar cells. Firstly, the LiPo battery was assumed to be at a reduced capacity during the test, providing energy between 14.8V and 12.0V dc before it was cut off. The power supply in the meantime was set with the same environments as in the previous case. Note that V1 (blue), V2 (red) and Vout (green).

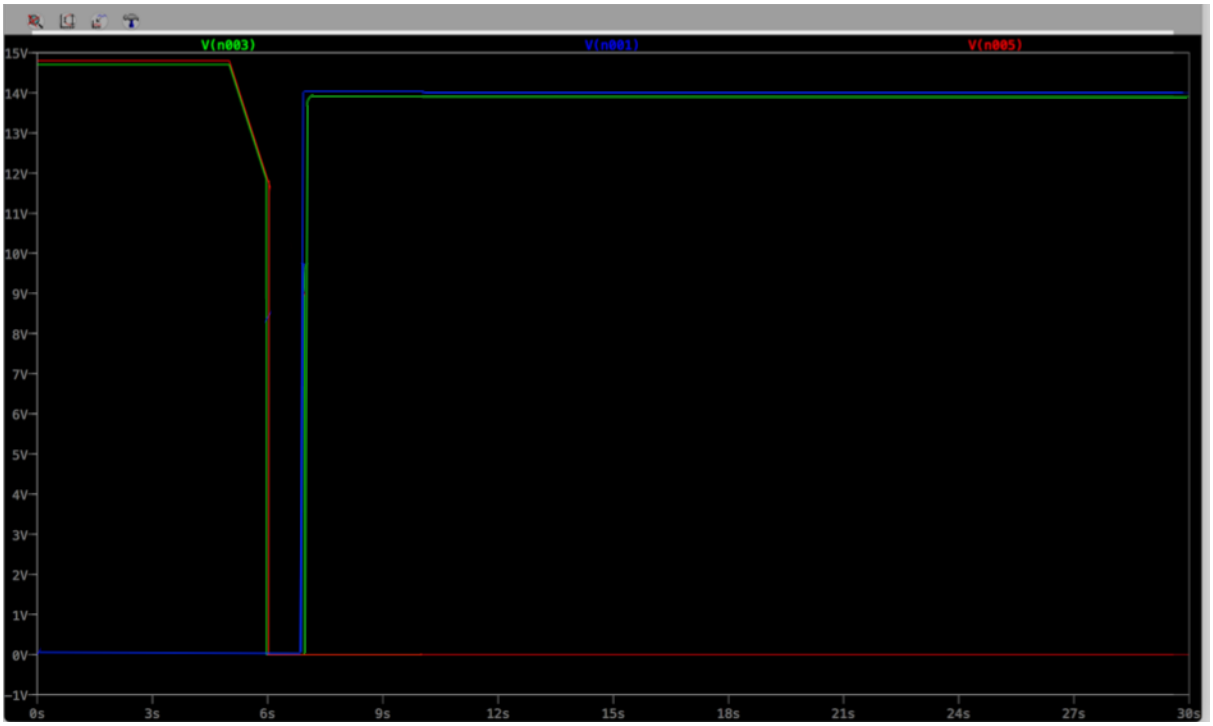

Figure 11: Line graph of resulting switch from battery to power supply

The result repeated the same situation experienced during the first case with Vout pulling less voltage than then the inputs. When V2 was disconnected at about 6.0s, the voltage droop in Vout was considerably longer than in case 1. The LTC4417 took some time to validate the V1 pin. Upon closer inspection it took about 500ms for the powerpath controller to accept the power supply as a valid input.

8. Discussions

Before discussing the obtained results, it is fair to know what the potential reasons for them are. Discussions were made with members of MAST to get different opinions and point of views about this project. First and foremost, in any experiment the real-world results will almost never be the same as the predicted theoretical results. There are many variables that must be controlled in order to get the best results possible. The author has defined two different types of variables that may have affected the project.

Controlled variables or constant variables were always assumed to remain the same throughout the whole project. Variables like the ambient temperature has changed quite drastically in the three months from May to July, which was the duration took to complete the project. All the calculations for the theoretical value were made at 25°C. The actual temperature was floating around 33°C at the highest and 20°C at the lowest. This may have had a direct impact on the performance of the circuitry. Some components like the MOSFETs have a sensitive power dissipation, P_D value at each temperature. The LTC4417 has at least seven parameters that are temperature sensitive, enhancing the seriousness of this issue. These parameters are;

i. Clamp voltage, V_G.
ii. Gate falling slew rate.
iii. Gate rising slew rate.
iv. Gate control low pull-down current, $I_{G(DN)}$.
v. Switchover time.
vi. Valid delay off time.
vii. $V_{OV(FALLING)}$ with $V_{UV(RISING)}$.

Resistance or internal resistance is another obvious variable in this project. Resistance comes from every single component used for this project. The resistance of connecting wires from the power supply and the multimeter was not considered in. The resistance coming from the PCB traces was assumed to be of the given value. In addition to that, the design of the PCB plays a role. The milling machine used has the smallest drilling separation of 0.1mm, while the LTC4417 has a distance of 0.2mm between the pads. Even the slightest error during the printing of the PCB will cause a short circuit in the chip, damaging it completely. Furthermore, the internal resistance of some components was not known from the beginning. The LiPo battery pack does not have any indication of its internal resistance online or on the battery pack itself. Not to mention that the calculation made was with the battery nominal charge of 3.7V per cell; an agreed convention by manufacturers to rate LiPo batteries. A fully charged battery would have up to 5-7 percent higher value.

Tolerances or variation in component values associated with manufactured components can increase the percentage of error and make a difference in the result. It is an unwelcome factor in the design of electronic circuits. The corresponding variations in circuit performance can often be great enough to cause the specifications of a circuit to be violated. Some appropriate corrective actions were established, although it is still worth noting that it can not be eradicated completely. These values stated above may be small and negligible, but they may add up quickly resulting in an unwanted increase in resistance.

The results of both tests were analysed and studied further. The most significant to note is that the voltage drop occurred in Vout which was the closest to the theoretical result. The Vout was not expected to pull out the exact same 14V or 14.8V. However, the voltage drop appeared to be better than expected. The author considers this part of the project successful as the energy efficiency of the circuit is very high.

Next, an analysis of the voltage droop. This is not the *forte* of the experiment. It is observed that the voltage droop during both tests were critical. In both cases, Vout was absent for a considerable amount of time. From the author's point of view, it is thought that the duration will be too long and unsafe for a real-world application.

9. Conclusions

The LTC4417 was the perfect choice for the idea of this project. As a powerpath controller it did its job well by transferring both power inputs to Vout. This all happened while the allowing the voltage inputs to be switched back and forth as seen in case 1 and 2. The author is satisfied to prove that this application can be used for the MASC. Voltage drop was minimal, revealing its high efficiency. However, the duration of the voltage droop is deemed too impactful for a higher level of application, referring to the MDH Solar Car. As the matter of fact, the absolute maximum voltage rating of the LTC4417 is 42V, much lower than the solar car's battery rated at 120V. A higher rated powerpath controller was not chosen by the author since it was known from the beginning that the solar car could not be tested on. There are many more considerations to be done when the solar car will be used during the 2019 Bridgestone World Solar Challenge. This project has served as a testing platform and should be studied and carried out further in the future. More refinements are necessary, and the author would be delighted to know if this idea can be used for the solar car.

10. Future Work

The result of the project can be improved by taking into consideration more parameters. The variables must be monitored at all times to ensure the right measuring values at the right conditions. Another way is to also increase the quality of the components used (e.g. higher efficiency, lower tolerances). A MOSFET with a lower $R_{DS(ON)}$ will significantly increase the voltage drop in the circuitry as two of them are used in series. The author intended to use IRF7324 with 18mΩ rated $R_{DS(ON)}$, however the component was not sold by the suppliers. Further testing is required to reduce the voltage droop. Better electrolytic capacitors with low ESR will be greatly appreciated.

For the application of pass through charging at a higher voltage level, an insulated-gate bipolar transistor (IGBT) or a power MOSFET would fit in. They act quite in a similar way to the a Powerpath Controller. Each has its own advantages over the other. In general, high voltage, high current and low switching frequencies favor the IGBT while low voltage, low current and high switching frequencies are the domain of the power MOSFET. Nonetheless, additional research and tests have to be carried out ensuring reliability of the system.

11. References and datasheets

[1]. https://www.worldsolarchallenge.org

[2]. http://blog.ravpower.com/2017/10/danger-and-damage-of-pass-through-technology-for-batteries/

[3]. M. Sorensen, D. Colic, U. Åkesson, G. Carlstedt, "Mini Autonomous Solar Team, MAST," Summer Project, M.Sc. Engineering in Robotics, IDT, Mälardalen University, Sweden.

[4]. https://developer.nvidia.com/embedded/buy/jetson-tx2

[5]. http://www.ni.com/sv-se/shop/select/roborio-advanced-robotics-controller

[6]. https://en.wikipedia.org/wiki/Robot_Operating_System

[7]. https://www.elfa.se/Web/Downloads/_t/ds/ltc4417_eng_tds.pdf

[8]. http://www.analog.com/en/technical-articles/primer-on-powerpath-controllers-ideal-diodes-prioritizers.html

[9]. http://www.interfacebus.com/Logic_Design_Voltage_Droop.html

[10]. https://www.sunpower-uk.com/glossary/what-is-inrush-current/

[11]. https://en.wikipedia.org/wiki/Lithium_polymer_battery

[12]. W. Palm, M. Heidari, F. Fischer, D. Hedlund, A. Ramberg, "Solar Challenge 2017," Project in Advanced Embedded Systems, M.Sc. Engineering in Robotics, IDT, Mälardalen University, Sweden.

[13]. G.T. Samson, T.M. Undeland, P.J.S Vie, "Optimal Load Sharing Strategy in a Hybrid Power System," Institute for Energy and Technology, NTNU, Norway.

[14]. B.T. Irving, M.M. Jovanovic, "Analysis, design, and performance evaluation of droop current-sharing method," Power Electron. Lab., Delta Products Corp., Research Triangle Park, NC, USA.

[i] IRF7342 MOSFET
- http://www.irf.com/product-info/datasheets/data/irf7342.pdf

[ii] R&S HMC8043 Power Supply
- https://www.rohde-schwarz.com/us/product/hmc804x-productstartpage_63493-61542.html

[iii] Turnigy 5000mAh 4S 25C-35C 14.8V LiPo battery
- https://hobbyking.com/en_us/turnigy-battery-5000mah-4s-25c-lipo-pack-xt-90.html

[iv] Fluke 45 Digital Multimeter
- http://nubilight.nubicom.co.kr/upload/datasheet/flu_45.pdf

[v] Schottky diode
- http://se.farnell.com/diodes-inc/bat54/diode-schottky-sot-23/dp/9526480?st=BAT54

[vi] Electrolytic capacitors
- https://www.electron.com/electrolytic-capacitor-jamicon-skr101m1ee11m-p1314/

[vii] Capacitors
- http://www.farnell.com/datasheets/47534.pdf

[viii] ProtoMat 63 milling machine
- https://www.lpkfusa.com/products/pcb_prototyping/machines/protomat_s63/

Appendices

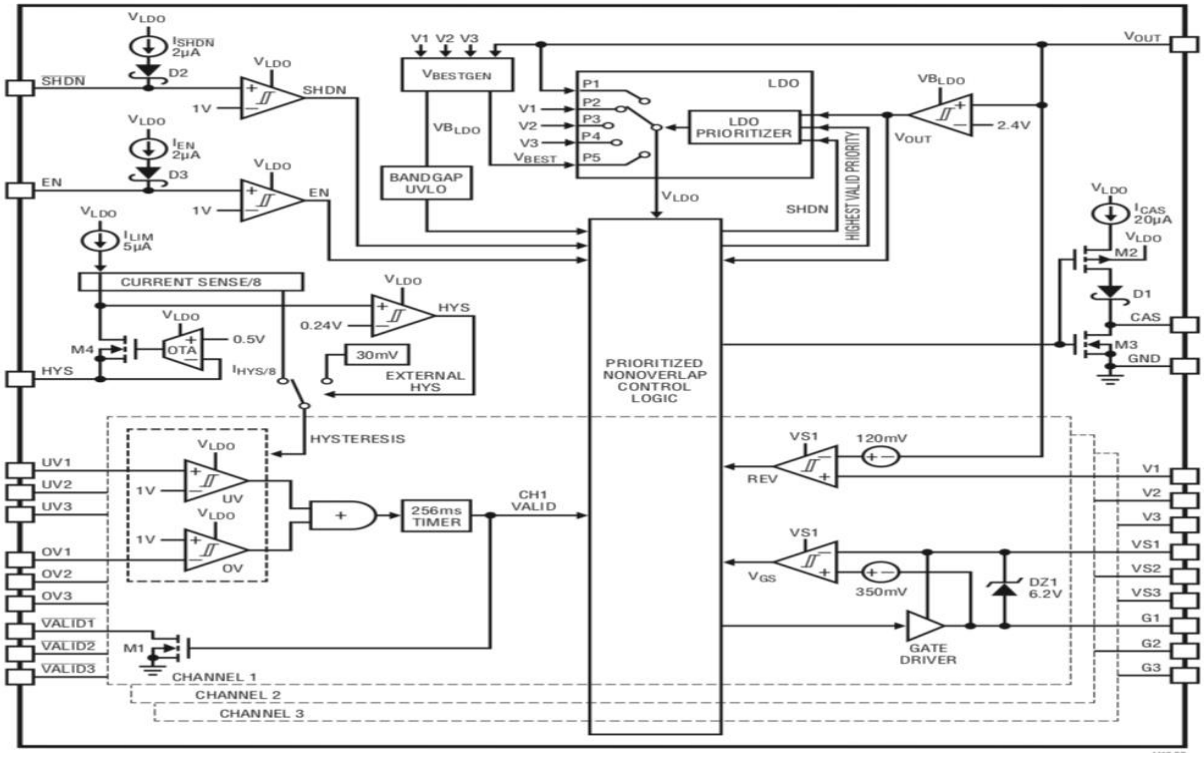

Appendix 1: Functional block diagram of the LTC4417

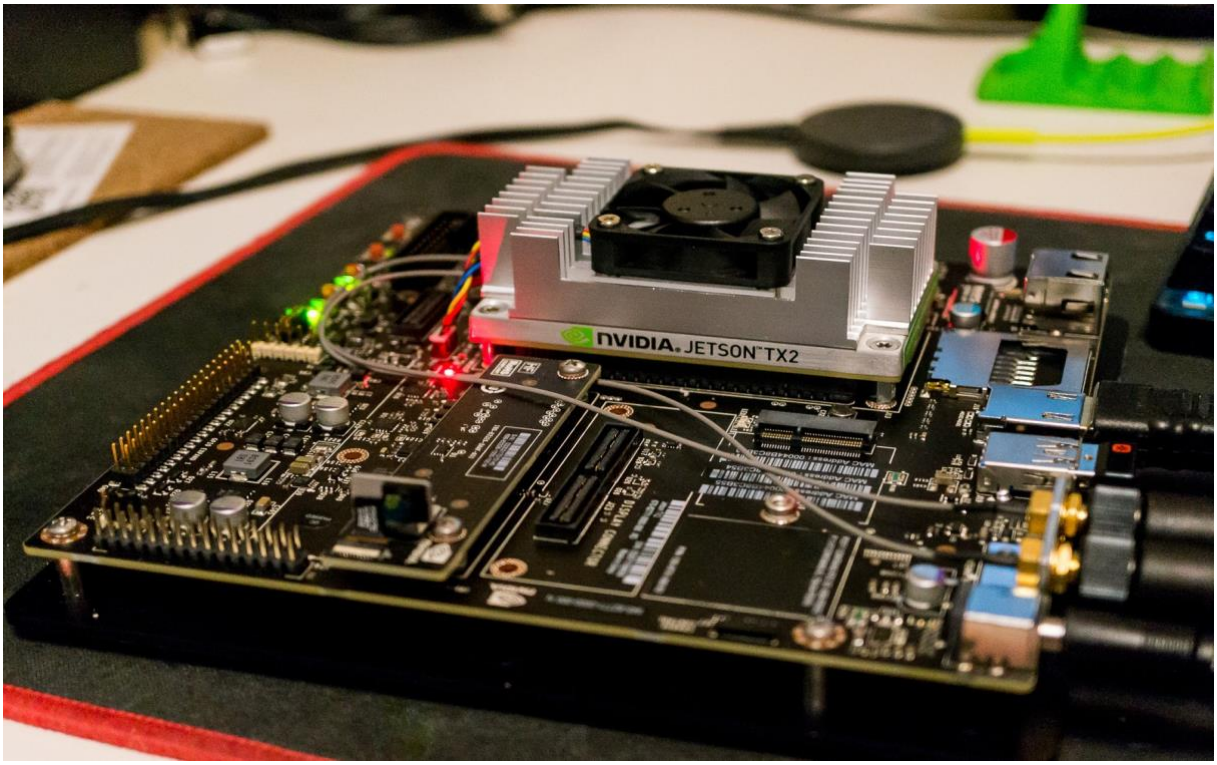

Appendix 2: NVIDIA Jetson TX2

Appendix 3: NI RoboRIO

Appendix 4: ProtoMat S63, the PCB milling machine

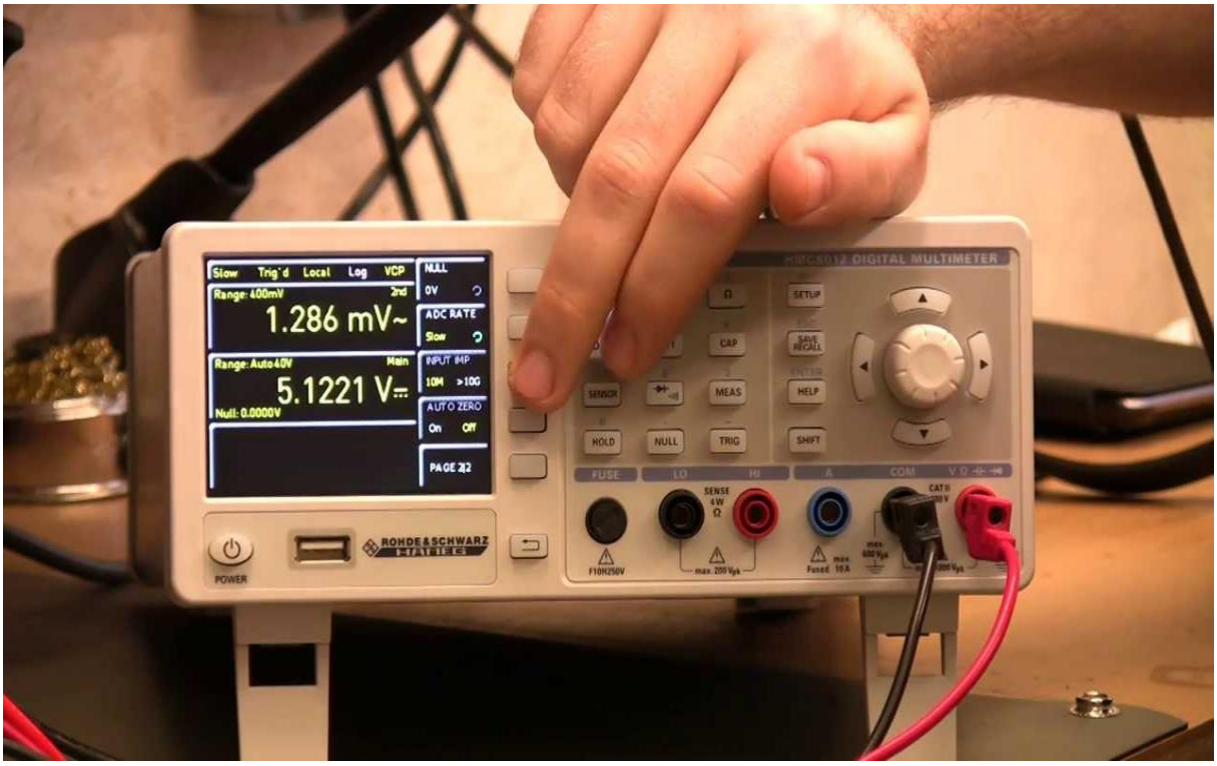

Appendix 5: R&S HMC8043 power supply

Appendix 6: Fluke 45 digital multimeter

Appendix 7: Turnigy 14.8V LiPo battery pack

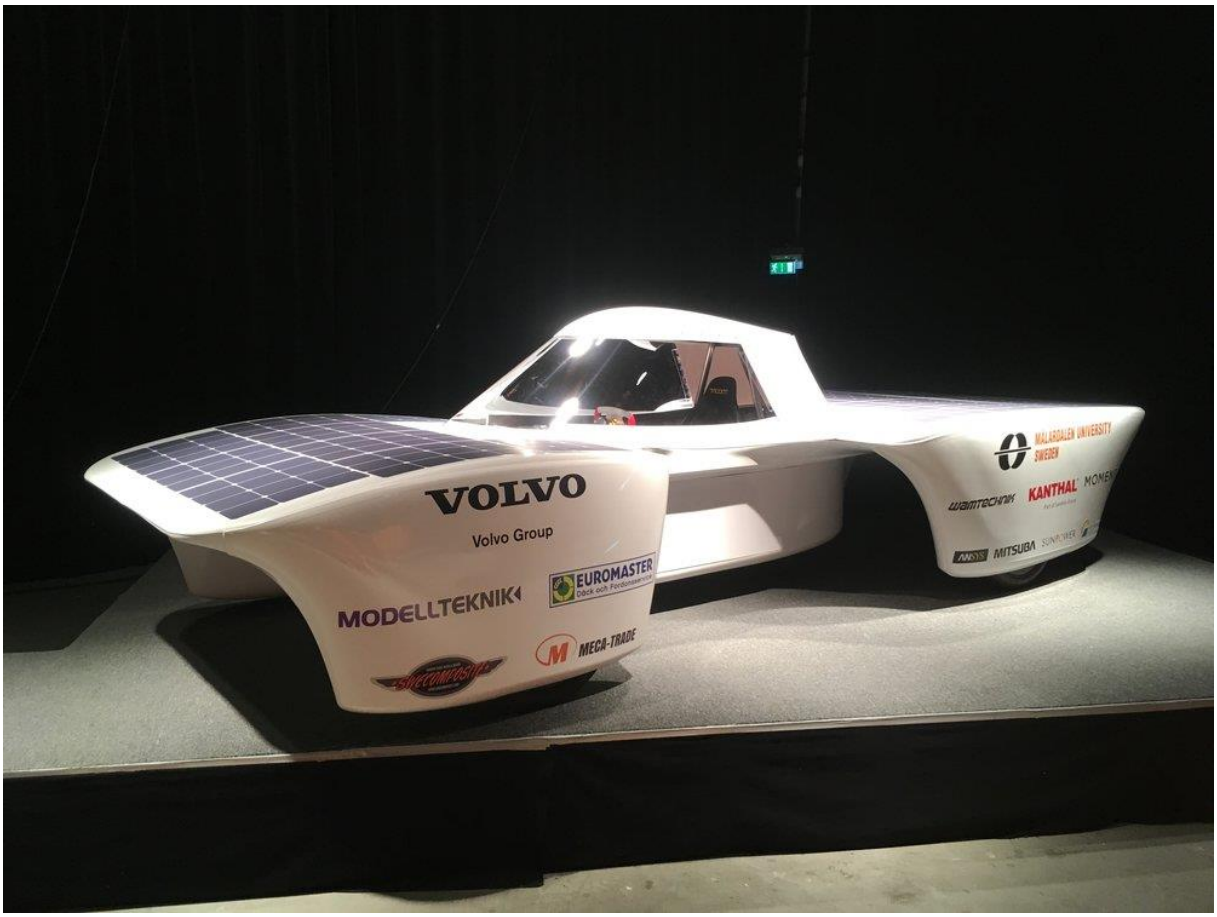

Appendix 8: MDH Solar Car

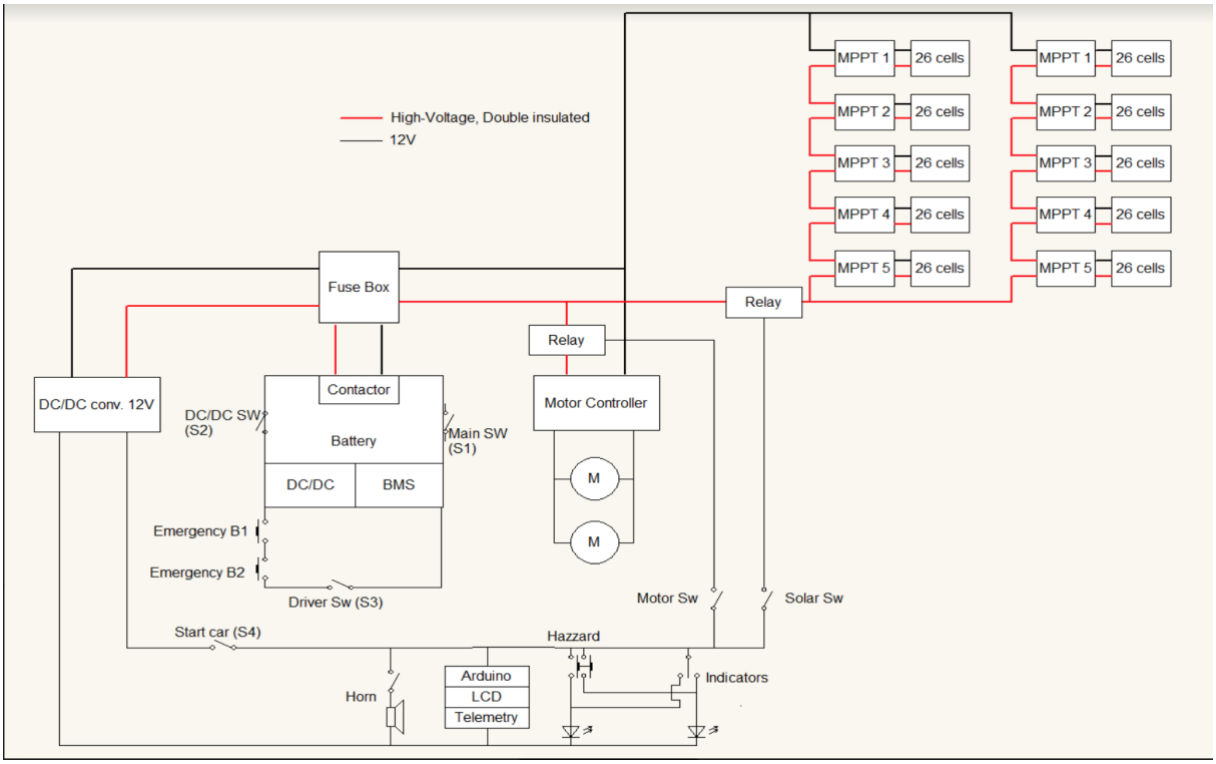

Appendix 9: Circuitry of the MDH Solar Car

Appendix 10: Battery pack of the MDH Solar Car

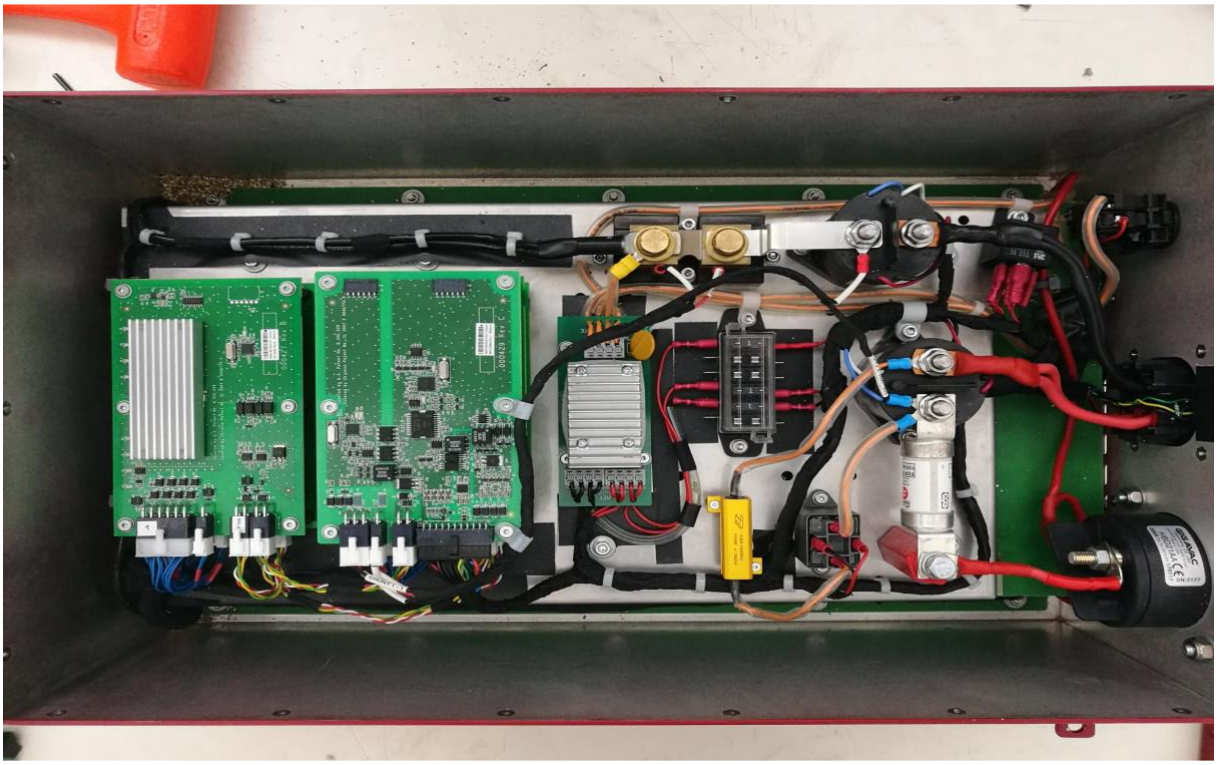

Appendix 11: Internal look of the battery pack

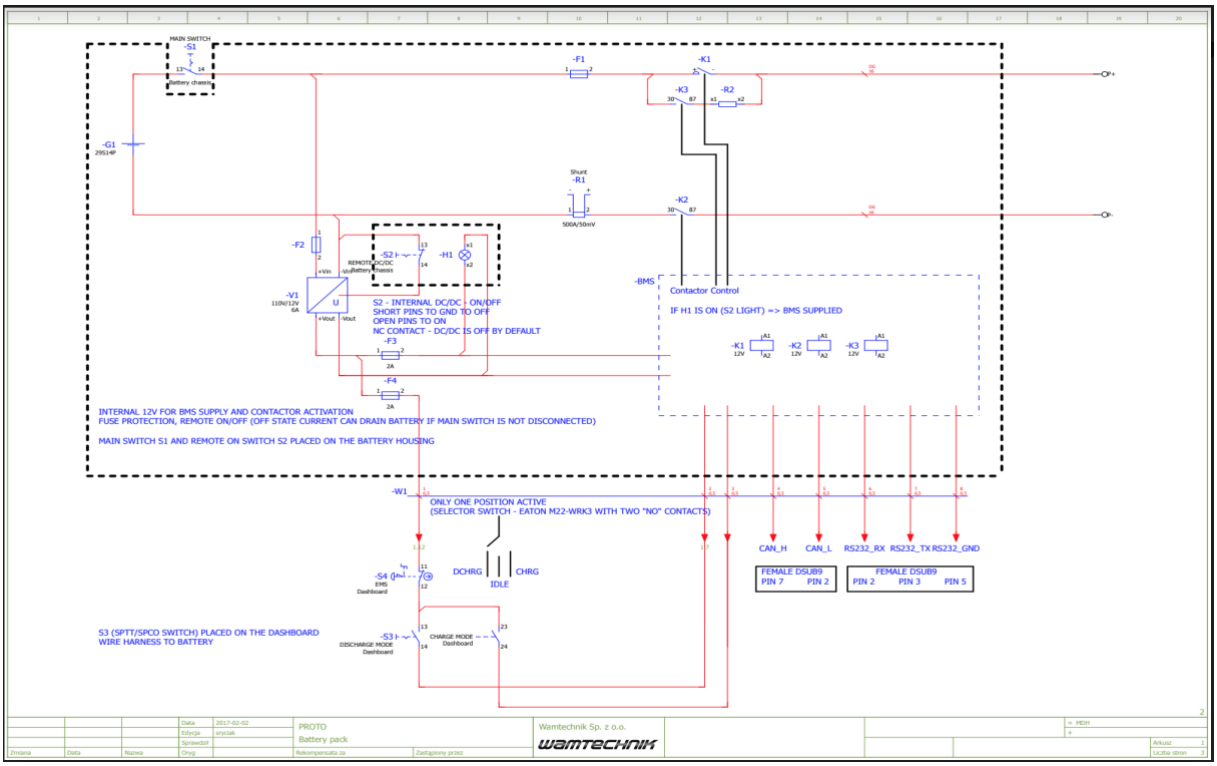

Appendix 12: Circuitry of the battery pack